

Chaos in Quantum Mechanics

by

Md. Mahfujur Rahman

16201012

Sovers Tonmoy pandey

16301029

A thesis submitted to the Department of Computer Science and Engineering
in partial fulfillment of the requirements for the degree of
B.Sc. in Computer Science

Department of Computer Science and Engineering
School of Data and Sciences
Brac University
January 2023

© 2023. Brac University
All rights reserved.

Declaration

It is hereby declared that

1. The thesis submitted is my/our own original work while completing degree at Brac University.
2. The thesis does not contain material previously published or written by a third party, except where this is appropriately cited through full and accurate referencing.
3. The thesis does not contain material that has been accepted or submitted for any other degree or diploma at a university or other institution.
4. We have acknowledged all main sources of help.

Student's Full Name & Signature:

Md. Mahfujur Rahman
16201012

Sovers Tonmoy pandey
16301029

Approval

The thesis/project titled “ Exploring the connection between quantum information, holography and the entropy of black holes.” submitted by

1. Md. Mahfujur Rahman(16201012)
2. Sovers Tonmoy pandey(16301029)

Of Fall, 2022 has been accepted as satisfactory in partial fulfillment of the requirement for the degree of B.Sc. in Computer Science on January 23, 2023.

Examining Committee:

Supervisor:
(Member)

Dr. Tibra Ali
Professor and Associate Dean
Department of Mathematics and Natural Sciences
Brac University

Program Coordinator:
(Member)

DR. Md.Golam Rabiul Alam
Professor
Department of Computer Science and Engineering
Brac University

Head of Department:
(Chair)

Sadia Hamid Kazi, PhD
Chairperson and Associate Professor
Department of Computer Science and Engineering
Brac University

Abstract

This thesis provides a detailed view of Out-of-time-order correlators in quantum mechanics. And how we can use OTOC to calculate chaos in quantum mechanics. We present precise OTOC calculations for a circle billiard, a particle in a one-dimensional box, a harmonic oscillator, and a stadium shape billiard. We will also take a brief look into chaos and quantum chaos.

Keywords: Chaos; Quantum Chaos; OTOC; classical Chaos ; Out-of-time-order correlators;

Dedication

We want to declare this research work to our parents, elder brother(Mahfujur) and my wife(Mahfujur) who have supported us greatly. We couldn't have achieved what we achieved without their support and motivation. We would also like to remember our friends and classmates who have challenged us to do better and who has shown their support whenever we needed it. Our supervisor, who has helped us throughout the years.

Acknowledgement

Firstly, all praise to the Great Allah for whom our thesis has been completed without any significant interruption.

Secondly, to our co-advisor, Dr Tibra Ali, sir, for his kind support and advice in our work. He helped us whenever we needed help.

And finally, to our parents, it may not be possible without their support. With their kind support and prayer, we are now on the verge of our graduation.

Table of Contents

Declaration	i
Approval	ii
Abstract	iii
Dedication	iv
Acknowledgment	v
Table of Contents	vi
List of Figures	viii
Nomenclature	ix
1 Introduction	1
1.1 Problem Statement	1
1.2 Research Objectives	1
2 Classical Chaos	3
2.1 History of Chaos Theory	3
2.2 Nonlinear Dynamics	3
2.3 Chaos	6
3 Quantum Chaos	8
3.1 History of Quantum Mechanics	8
3.2 Quantum chaos	8
4 OTOC	10
4.1 Classical Motivation	10
4.2 OTOC in Quantum Mechanics	11
4.3 The Harmonic Oscillator	13
4.4 Particle in a 1D box	17
5 OTOC-2	20
5.1 Circle Billiard	20
5.2 Stadium Billiard	26
5.3 Classical Statistics	29

6 Conclusion	40
Bibliography	41

List of Figures

2.1	The phase potential of (2.5), cf(2.4) [1]	4
2.2	The phase potential of (2.12), The shaded area shows the basin of attraction of the origin for $b > 0$. [1]	6
4.1	Microcanonical OTOC for Harmonic Oscillator [6]	16
4.2	Thermal OTOC for Harmonic Oscillator [6]	16
5.1	Implicit region of a circle	21
5.2	Mesh of a circle billiard	21
5.3	Eigenvalues of the circle billiard	24
5.4	Eigenfunction for $n = 1$ of circle billiard	25
5.5	Eigenfunction for $n = 2$ of circle billiard	26
5.6	Eigenfunction for $n=3$ of circle billiard	27
5.7	Eigenfunction for $n = 6$ of circle billiard	28
5.8	Eigenfunction for $n = 10$ of circle billiard	29
5.9	Eigenfunction for $n = 50$ of circle billiard	30
5.10	Eigenfunction for $n = 100$ of circle billiard	31
5.11	Eigenfunction for $n = 200$ of circle billiard	31
5.12	Eigenfunction for $n = 400$ of circle billiard	32
5.13	3D view for $n = 400$ in circle billiard	32
5.14	Trajectory of stadium billiard	33
5.15	Positive Lyapunov exponent	33
5.16	Mesh of stadium billiard	33
5.17	Eigenvalues of stadium billiard	34
5.18	Eigenfunction for $n=1$ of stadium billiard	34
5.19	Eigenfunction for $n=2$ of stadium billiard	35
5.20	Eigenfunction for $n=3$ of stadium billiard	35
5.21	Eigenfunction for $n=10$ of stadium billiard	36
5.22	Eigenfunction for $n=50$ of stadium billiard	36
5.23	Eigenfunction for $n=100$ of stadium billiard	37
5.24	Eigenfunction for $n=200$ of stadium billiard	37
5.25	Eigenfunction for $n=400$ of stadium billiard	38
5.26	3D view for $n= 400$ in stadium billiard	38
5.27	OTOC for Stadium billiard	39
5.28	OTOC for Stadium billiard	39

Nomenclature

The next list describes several symbols & abbreviation that will be later used within the body of the document

OTOC Out-of-time-order

Chapter 1

Introduction

1.1 Problem Statement

Chaos theory and quantum mechanics are two of the most significant part of modern physics. Chaos theory discusses the random and unpredictable behavior of a dynamic system. The systems are sensitive to the initial state, which can lead to drastically different results.

Quantum mechanics is a fundamental theory in physics that describes the behavior of matter and energy at the atomic and subatomic scales. It is based on wave-particle duality and uncertainty principles, representing the dual nature of matter and energy and the inherent uncertainty in our ability to measure them.

In quantum mechanics, the wave function represents the particles' behaviors, representing the probability of finding a particle at a particular location in space [2]. The Schrödinger equation governs these wave functions,

$$i\hbar \frac{d}{dt} |\Psi(t)\rangle = \hat{H} |\Psi(t)\rangle \quad (1.1)$$

In this equation, Ψ represents the time-dependent wave function, and \hat{H} represents the Hamiltonian operation.

In quantum mechanics, chaotic systems are characterized by quantum states that are highly sensitive to perturbations or changes in their initial conditions. This means that small changes in the initial conditions of a chaotic system can lead to significant differences in its behavior over time.

One of the critical features of chaotic systems in quantum mechanics is the presence of quantum chaos or the "chaos" associated with the quantum states of these systems. This is characterized by high randomness, unpredictability in the system's behavior, and a sensitivity to perturbations.

1.2 Research Objectives

One of the ways we can measure quantum chaos is the out-of-time-order correlator(OTOC). In this thesis, we will look into measuring OTOC for quantum mechanics. We will also look into the fundamentals of classical chaos and nonlinear dynamics, how chaos is generally derived, and how it works. Then we will look

into chaos in quantum mechanics and different kind of chaotic behavior in quantum mechanics. We will further discuss how to measure OTOC on a particle in a one-dimensional box, a circle billiard and a stadium billiard.

Chapter 2

Classical Chaos

2.1 History of Chaos Theory

The origins of chaos theory can be traced back to the work of French mathematician Henri Poincaré in the late 19th century. Poincaré studied the three-body problem in celestial mechanics, which involves predicting the motion of three celestial objects (such as planets or asteroids) interacting with each other. He discovered that even minor differences in the initial positions and velocities of the objects could lead to vastly different outcomes, making the problem impossible to solve.

In the 1940s and 1950s, mathematician John von Neumann and meteorologist Edward Lorenz developed mathematical models to study weather patterns and the behavior of complex systems. Lorenz discovered that small changes in the initial conditions of his weather model could lead to drastically different weather patterns over time, a phenomenon that came to be known as the butterfly effect.

In the 1960s and 1970s, several mathematicians and physicists, including James Yorke, Tien-Yien Li, and James Gleick, made significant contributions to the development of chaos theory. They introduced new mathematical tools and techniques for studying chaotic systems and developed the concept of fractals, which are self-similar geometric shapes that exhibit complexity at all scales.

In the 1980s and 1990s, chaos theory continued to be developed and applied to various fields, including physics, biology, economics, and computer science.

What does chaos refer to? In physics, chaos refers to the behavior of a dynamic system susceptible to initial conditions, meaning that minor differences in initial conditions can lead to vastly different outcomes over time. This behavior is characteristic of chaotic systems, which exhibit seemingly random and unpredictable behavior.

2.2 Nonlinear Dynamics

Nothing in this universe is indeed linear. Everything that exists in nature is nonlinear. From the earth's surface to ocean movement to animal movement, nothing is genuinely linear, but we still try to understand nature using linear approximation. Let us look into a simple harmonic oscillator, a spring with a mass of m attached

where the force increases linearly in the displacement $x(t)$,

$$m \frac{d^2x}{dt^2} = -kx \quad (2.1)$$

Here k represents the spring constant which is greater than 0. This model will give accurate results under most conditions. But if we look at equation (2.1) it lets us stretch the spring to whatever length we want to and not break it or change its spring nature or the constant. This is invalid, so nonlinearity is added to make the model more realistic. So, equation (2.1) becomes,

$$\frac{d^2x}{dt^2} = -\omega_o^2 x + x^2 \quad (2.2)$$

The ω_o^2 represents k/m in the equation. No extra parameters are added before the nonlinear terms, as those could be removed by increasing x at a constant rate.

The difference between (2.1,2) is that more equilibrium points are not just $x = 0$. Now, if we consider the right-hand side of equation (2.2) zero, we will find the two points of equilibrium,

$$\bar{x} = 0, \quad \bar{x} = \omega_o^2 \quad (2.3)$$

We can check the dynamics near these points to understand the necessity and significance of this set of points.

If we multiply (2.2) with dx/dt and integrate it once we get,

$$\frac{1}{2}y^2 + \frac{1}{2}\omega_o^2 x^2 - \frac{1}{3}x^3 = \text{const} = E \quad (2.4)$$

We replaced dx/dt with y . This equation is the integral of motion, and E represents the system's total energy. We can also write equation (2.2) as their first-order ordinary differential equations (ODEs),

$$\begin{aligned} \frac{dx}{dt} &= y \\ \frac{dy}{dt} &= -\omega_o^2 x + x^2 \end{aligned} \quad (2.5)$$

using equation (2.4), we can plot for different values of E on the (x,y) phase plane. We will get fig. 1 after we plot the graph.

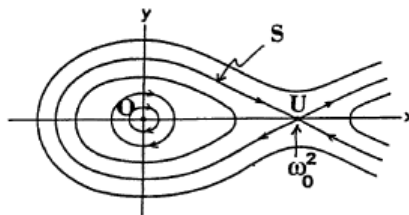


Figure 2.1: The phase potential of (2.5), cf(2.4) [1]

From fig.2.1, we can see the curve S where $E = E_o = \omega_o^2/6$. This is known as the separatrix. This is the bound beyond which the oscillatory motion escapes to infinity. Inside this S curve, the spring behaves like a harmonic oscillator. We can now linearize the (2.5) about the fixed point U,

$$x(t) = \bar{x} + \xi(t), \quad y(t) = \bar{y} + \eta(t) \quad (2.6)$$

with $(\bar{x}, \bar{y}) = (\omega_o^2, 0)$ we get,

$$\begin{bmatrix} \dot{\xi} \\ \dot{\eta} \end{bmatrix} = \begin{bmatrix} 0 & 1 \\ \omega_o^2 & 0 \end{bmatrix} \begin{bmatrix} \xi \\ \eta \end{bmatrix} = L \begin{bmatrix} \xi \\ \eta \end{bmatrix} \quad (2.7)$$

Here $(\dot{\quad})$ represents $d()/dt$. Now, if we find the eigenvalues and eigenvectors of L:

$$\lambda_1 = -\omega_o, \quad \lambda_2 = \omega_o, \quad e_1 = \begin{bmatrix} 1 \\ -\omega_o \end{bmatrix}, \quad e_2 = \begin{bmatrix} 1 \\ \omega_o \end{bmatrix} \quad (2.8)$$

For $\{e_1, e_2\}$, the general solution near U is,

$$\frac{1}{2}(\xi(0) - \omega_o^{-1}\eta(0))e^{-\omega_o t}e_1 + \frac{1}{2}(\xi(0) + \omega_o^{-1}\eta(0))e^{\omega_o t}e_2 \quad (2.9)$$

Equation (2.9) elaborates on the measurable idea near U in fig.2.1. Here, U is known as the saddle-node, which is always unstable. If we do linearization near the origin, we will find stable solutions. O is known as the center point.

Now, if we add dampening, which is relative to the velocity, to make equation (1.2) more real life we get,

$$\ddot{x} = -\omega_o^3 x - b\dot{x} + x^2, \quad b > 0 \quad (2.10)$$

As we can see, equation (2.10) is non-integrable. It has now become a nonconservative system, which is called dissipative where area $\Delta A = \Delta x \Delta y$, everywhere in (x,y) phase space, the time evolution of the dissipate is,

$$\begin{aligned} \frac{d}{dt}(\Delta A) &= (\Delta x \Delta y) \left[\frac{1}{\Delta x} \frac{d\Delta x}{dt} + \frac{1}{\Delta y} \frac{d\Delta y}{dt} \right] = (\Delta A) \left[\frac{\Delta \dot{x}}{\Delta x} + \frac{\Delta \dot{y}}{\Delta y} \right] \\ &\xrightarrow[\Delta x \rightarrow 0, \Delta y \rightarrow 0]{} (\Delta A) \left[\frac{\partial \dot{x}}{\partial x} + \frac{\partial \dot{y}}{\partial y} \right] = -b(\Delta A) \end{aligned} \quad (2.11)$$

here $(\Delta A) \propto (-bt)$ The last part of (2.11) can be done after writing (2.10) as a system of,

$$\begin{aligned} \dot{x} &= y = f_1(x, y) \\ \dot{y} &= -\omega_o^2 x - by + x^2 = f_2(x, y) \end{aligned} \quad (2.12)$$

In a broader sense, we can say that the quantity determines the system of the form (2.12) for the rate of change in elementary areas.

$$\nabla \cdot f = Tr[Df(x, y)] = \frac{\partial f_1}{\partial x} + \frac{\partial f_2}{\partial y} \quad (2.13)$$

Here, the trace is represented by Tr, and Df is the Jacobin matrix of $f \equiv (f_1, f_2)$,

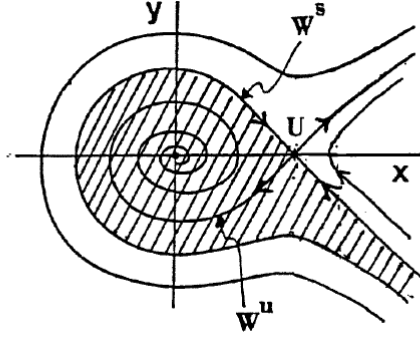


Figure 2.2: The phase potential of (2.12), The shaded area shows the basin of attraction of the origin for $b > 0$. [1]

$$Df(x, y) = \begin{bmatrix} \frac{\partial f_1}{\partial x} & \frac{\partial f_1}{\partial y} \\ \frac{\partial f_2}{\partial x} & \frac{\partial f_2}{\partial y} \end{bmatrix} (x, y) \quad (2.14)$$

The behavior of orbits in the (x, y) phase plane for $b < 2\omega_o$ is revealed by a linear analysis at the fixed points of (2.12); see figure 2. The direction field $dy/dx = (-\omega^2 x - by + x^2)/y$ at various points (x, y) , and geometric considerations demonstrate that The separatrix S in Figure 1 has been divided into two curves, designated as the stable and unstable manifolds of the saddle fixed point at U, respectively, by the letters W^s and W^u . The steady focal point at the origin of O's basin of attraction is indicated by the shaded area in Figure 2. This basin gradually expands with increasing b (stronger damping) and contracts with decreasing b (positive b). For $b = 0$, it entirely vanishes since the origin, while steady, is not an attractor anymore because the origin is an unstable fixed point when $b < 0$, and the basin surrounding O does not exist.

Equations (2.1) and (2.7) are examples of linear equations. And (2.2), (2.5), and (2.12) are nonlinear equations.

2.3 Chaos

From nonlinear dynamics can formulate that chaos is fundamentally self-similar under scaling, and it is susceptible to changes in the initial conditions.

The self-similar nature offers the reassuring insight that, even though an item may appear complex at first glance, its complexity may result from the superposition of patterns that become self-similar at the limit of infinite magnification.

To calculate chaos, we measure the rate of exponential separation of trajectories, as determined by Lyapunov exponents of the orbits in various phase space directions; for simplicity's sake, let's focus on one-dimensional maps.

$$x_{n+1} = f(x_n), \quad x_n \in R \quad (2.15)$$

For the initial condition, we can write the equation as,

$$x_n = f^n(x_o) \quad (2.16)$$

Let's say we want to follow a nearby orbit, beginning at $x'_o = x_o + \xi$ where ξ is small,

$$x'_n = f^n(x_o + \xi) \quad (2.17)$$

Now we observe the evolution of the separation between these orbits over time,

$$|f^n(x_o + \xi) - f^n(x_o)| \propto \xi e^{\lambda(x_o)n}, \quad n \gg 1 \quad (2.18)$$

The speed at which these two orbits diverge is $\lambda(x_o)$, which is the Lyapunov exponent. When $n \rightarrow \infty$ and $\xi \rightarrow 0$ we can get,

$$\begin{aligned} \lambda(x_o) &= \lim_{n \rightarrow \infty} \frac{1}{n} \log \left| \frac{df^n(x_o)}{dx_o} \right| \\ &= \lim_{n \rightarrow \infty} \frac{1}{n} \sum_{i=0}^n \log |f'(x_i)| \end{aligned} \quad (2.19)$$

When $\lambda(x_o) > 0$ and there are vast initial conditions, the orbits we will get will show some chaotic nature. On the other hand, when $\lambda(x_o) < 0$, the orbits are anticipated to converge to a regular attractor.

There are m Lyapunov exponents in m -dimensional dynamical systems. The greatest one $\lambda_{max} = \max(\lambda_i : 1 \leq i \leq m)$, which specifies the rate at which the norm of the distance between close trajectories increases in time, is what we are often interested in. In a region $D \in R$, if $\lambda_{max} > 0$ and is independent of $x(0)$, chaotic behavior with statistical characteristics common to the majority of orbits in that region are observed [1].

Chapter 3

Quantum Chaos

3.1 History of Quantum Mechanics

Quantum mechanics offers a mathematical foundation for comprehending the behavior of particles at the atomic and subatomic scales. It was created in the early 20th century and has significantly influenced how we perceive the nature of matter and energy.

Generally, there are two significant periods for quantum mechanics the early development of the theory in the 1920s and its further growth and implementation in the decades.

The discovery of the atomic nucleus and the advancement of the nuclear theory is closely related to the early development of quantum mechanics. Early in the 1900s, researchers like Ernest Rutherford and Niels Bohr made significant contributions to our understanding of the atomic structure and put forth theories that explained how atomic spectra behaved.

With the work of physicists like Max Planck, Albert Einstein, Werner Heisenberg, and Erwin Schrödinger, quantum mechanics emerged as a complete theory in the 1920s. These researchers made several ground-breaking findings that helped quantum mechanics become a foundational theory of matter and energy.

The key feature of quantum mechanics is that particles can behave like a particle and a wave depending on how they are observed.

3.2 Quantum chaos

Defining quantum chaos is not easy to solve. Since the early days of quantum mechanics, the development of quantum chaos has been present, and it is still under development.

From classical chaos, we know the system has to be highly dependent and sensitive to the initial condition to be considered chaotic. To understand the trajectory of a particle, we would have to know the $x(t)$ and $p(t)$, which are the position and momentum of the particle. But from the Heisenberg uncertainty principle, we know that it is impossible to measure the velocity and position of a particle at the same time. If we accurately measure the position's value, we don't know anything about the momentum and vice versa, which means that classical chaos is incompatible with Quantum mechanics. That is why quantum chaos is a complex problem to determine.

In the upcoming chapter, we will find chaos by using operators instead of states and calculating the OTOCs.

Chapter 4

OTOC

The primary computational methods for determining whether a quantum system is chaotic are presented in this chapter, as well as the concept of quantum chaos. At the end of this chapter, we provide a brief summary of the findings that will be presented in the subsequent chapters.

4.1 Classical Motivation

Since the improvement of quantum mechanics, the investigation of quantized portrayals of traditional frameworks has been a focal issue in physics. One way to transition from classical physics to quantum mechanics is through the Poisson bracket. Regarding a classical system with a generalized position $x(t)$ and corresponding momentum $p(t)$, the Poisson bracket $\{..., ..\}_{x(t),p(t)}$

$$\{A, B\}_{x(t),p(t)} = \frac{\partial A}{\partial x(t)} \frac{\partial B}{\partial p(t)} - \frac{\partial A}{\partial p(t)} \frac{\partial B}{\partial x(t)} \quad (4.1)$$

where A and B are any x and p -related functions. The commutator $[.., ..]$ of operators must be related to the Poisson bracket in order to enter the quantum domain.

$$[\hat{A}, \hat{B}] = i\hbar\{A, B\}_{x,p} \quad (4.2)$$

$$[\hat{A}, \hat{B}] = \hat{A}\hat{B} - \hat{B}\hat{A} \quad (4.3)$$

Here, the quantum equivalents of the classical quantities A and B are represented by the Hermitian operators \hat{A} and \hat{B} . The time-dependent Heisenberg operators $\hat{A}(t)$, which are connected to the time-independent Schrödinger operators $\hat{A} = (\hat{A}(0))$ and Hamiltonian \hat{H} is time independent.

$$\hat{A}(t) = \hat{A}e^{i\hat{H}t}e^{-i\hat{H}t} \quad (4.4)$$

Understanding quantum chaos is the current objective. Utilizing Equation 4.2 and 4.3 to comprehend the quantum analogue of classical chaos by relating it to a Poisson bracket is one method for resolving the issue. A chaotic system classically exhibits extreme sensitivity to the initial conditions. Consider two classical particles in one dimension whose locations are $x_1(t)$ and $x_2(t)$, the initial condition is,

$$\delta_x(t) = x_1(0) - x_2(0) \quad (4.5)$$

where $\delta_x(t)$ is very tiny than 1. The system will be chaotic if the initial behavior is,

$$\delta_x(t) = \delta_x(0)e^{\lambda_L t} \quad (4.6)$$

that is, the increase in the particle positions' differences is exponential. The system's Lyapunov exponent is represented by the constant λ_L .

4.2 OTOC in Quantum Mechanics

The OTOC is generally represented as,

$$C_T(t) \equiv - \langle [\hat{x}(t), \hat{p}(0)]^2 \rangle \quad (4.7)$$

Here, \hat{x} and \hat{p} are represent position and momentum operator in time-independent Hamiltonian phase space respectively.

This is demonstrated for quantum mechanical systems that are defined by a discrete spectrum Hamiltonian. Due to the fact that discrete spectra are simpler to work with than continuous spectra and quantum mechanical calculations are typically much simpler than quantum field theory calculations, this is a great place to start when exploring the many behaviors of OTOC.

The system is in E_n energy state and the density operator is classically,

$$\rho = \frac{e^{-\frac{E}{K_B T}}}{Z}$$

Where,

$$Z = \int dE e^{-\frac{E}{K_B T}}$$

This is called as partition function.

Now, we use the eigenstate $|E_n\rangle$ of Hamiltonian to define $C_T(t)$

$$C_T(t) = \frac{\sum_n \langle E_n | - [\hat{x}(t), \hat{p}(0)]^2 e^{-\frac{H}{K_B T}} | E_n \rangle}{\sum_n \langle E_n | e^{-\frac{H}{K_B T}} | E_n \rangle} \quad (4.8)$$

We can define $\frac{1}{K_B T} = \beta$

$$C_T(t) = \frac{\sum_n \langle E_n | - [\hat{x}(t), \hat{p}(0)]^2 e^{-\beta H} | E_n \rangle}{\sum_n \langle E_n | e^{-\beta H} | E_n \rangle}$$

or,

$$C_T(t) = \frac{\sum_n e^{-\beta H} \langle E_n | - [\hat{x}(t), \hat{p}(0)]^2 | E_n \rangle}{\sum_n \langle E_n | e^{-\beta H} | E_n \rangle}$$

or,

$$C_T(t) = \frac{\sum_n e^{-\beta H} C_n(t)}{\text{Tr} e^{-\beta H}} \quad (4.9)$$

We know, $\text{Tr} e^{-\beta H} = Z$ which is partition function. So, equation 4.9 implies as,

$$C_T(t) = \frac{1}{Z} \sum_n e^{-\beta H} C_n(t) \quad (4.10)$$

Here, $C_T(t)$ is thermal average of all of microcanonical OTOC and $C_n(t)$ is micro-canonical OTOC,

$$C_n(t) = \langle E_n | - [\hat{x}(t), \hat{p}(0)]^2 | E_n \rangle \quad (4.11)$$

Inserting an entire set of energy eigenstates $\hat{E} = \sum_n |E_n\rangle \langle E_n|$ is the following stage in the process of discovering an usable form for the OTOC. So, from equation 4.11 we get,

$$C_n(t) = \sum_m b_{nm}(t) b_{nm}^*(t) \quad (4.12)$$

And,

$$b_{nm} = -i \langle E_n | [\hat{x}(t), \hat{p}(0)] | E_m \rangle \quad (4.13)$$

$b(t)$ is a Hermitian matrix. So,

$$b_{nm} = -i \langle E_n | [\hat{x}(t), \hat{p}(0)] | E_m \rangle$$

$$b_{mn} = i \langle E_n | [\hat{x}(t), \hat{p}(0)] | E_m \rangle = b_{nm}^*$$

From equation 4.13 we get,

$$b_{nm} = -i \langle E_n | [\hat{x}(0), \hat{p}(0)] | E_m \rangle$$

$$b_{nm} = \left\langle E_n | e^{i\hat{H}t} \hat{x}(0), \hat{p}(0) e^{-i\hat{H}t} | E_m \right\rangle$$

$$b_{nm} = \sum_k e^{i(E_n - E_k)t} x_{nk} p_{km} \quad (4.14)$$

Here,

$$x_{nk} = \langle E_n | \hat{x}(0) | E_k \rangle$$

And,

$$p_{km} = \langle E_k | \hat{p}(0) | E_m \rangle$$

Finally, equation 4.13 and 4.14 give us,

$$b_{nm} = -i \sum_k (e^{i(E_n - E_k)t} x_{nk} p_{km} - e^{i(E_k - E_m)t} p_{nk} x_{km}) \quad (4.15)$$

It would be preferable to formulate Equation 4.15 only using the matrix elements of \hat{x} because they are considerably simpler to manipulate numerically. If the Hamiltonian is,

$$\hat{H} = \frac{1}{2} \hat{p}^2 + v(\hat{x}) \quad (4.16)$$

SO, $[\hat{H}, \hat{x}] = \frac{1}{2} [\hat{p}^2, \hat{x}] = -i\hat{p}$ and matrix elements,

$$p_{nm} = i(E_n - E_m) x_{nm} \quad (4.17)$$

After plugging this value on equation 4.15,

$$b_{nm}(t) = \frac{1}{2} \sum_k x_{nk} x_{kn} (E_{km} e^{iE_{nk}t} - E_{nk} e^{iE_{km}t}) \quad (4.18)$$

4.3 The Harmonic Oscillator

The Hamiltonian of simple harmonic oscillation is define by [6],

$$H = \frac{p^2}{2m} + \frac{1}{2} kx^2 \quad (4.19)$$

here, k is the force constant is must be greater than zero. Let us assume, the form of classical and quantum Hamiltonian are the same then time independent Schrodinger is written as,

$$\frac{d^2\psi}{dx^2} = \frac{2m}{\hbar^2} \left(\frac{1}{2} kx^2 - E \right) \psi \quad (4.20)$$

Where,

m = mass of the particle

E = Energy

We know, the classical angular frequency,

$$\omega = \sqrt{\frac{k}{m}}$$

or,

$$k = \omega^2 m$$

Let,

$$y = \sqrt{\frac{m\omega}{\hbar}} x$$

or,

$$x^2 \frac{m\omega}{\hbar} = y^2$$

or,

$$x^2 = \frac{y^2 \hbar}{m\omega}$$

Further let,

$$\epsilon = \frac{2E}{\hbar\omega}$$

or,

$$E = \frac{\epsilon \hbar \omega}{2} \quad (4.21)$$

After substituting these value on equation 4.20 we get,

$$\frac{d^2\psi}{dy^2} = (y^2 - \epsilon)\psi$$

or,

$$\frac{d^2\psi}{dy^2} - (y^2 - \epsilon)\psi = 0 \quad (4.22)$$

boundary condition of 4.22 is $\psi \rightarrow 0$ as $|y| \rightarrow \infty$ and after simplify 4.22 we get,

$$\frac{d^2\psi}{dy^2} - y^2\psi = 0 \quad (4.23)$$

The solutions of equation 4.23 are,

$$\psi(y) = A(y)e^{\pm \frac{y^2}{2}}$$

where $A(y)$ is a function of y that changes very slowly. $A(y)$ is a decaying solution.

$$\psi(y) = h(y)e^{-\frac{y^2}{2}}$$

By putting this value on equation 4.22, we obtain,

$$\frac{d^2h}{dy^2} - 2y \frac{dh}{dy} + (\epsilon - 1)h = 0 \quad (4.24)$$

The power-low solution,

$$h(y) = \sum_{n=0}^{\infty} c_n y^n \quad (4.25)$$

From equation 4.24 and 4.25

$$c_{i+2} = \frac{2i - \epsilon + 1}{(i+1)(i+2)} c_i \quad (4.26)$$

y is dominator at large $|y|$ and higher power of y ,

$$h(y) = C \sum_i \frac{y^{2i}}{i!}$$

or,

$$h(y) = C e^{y^2} \quad (4.27)$$

From equation 4.25 and 4.26,

$$\epsilon = 2n + 1$$

After put this value on equation 4.21 we get [5],

$$E = (n + \frac{1}{2}) \hbar \omega$$

$$E_n = (n + \frac{1}{2}) \hbar \omega \quad (4.28)$$

Here, $n = 0, 1, 2, 3, \dots$

WE can rewrite the equation 4.23 as

$$\psi_n \left(-\frac{d^2}{dy^2} + y^2 \right) = \psi_n (2n + 1) \quad (4.29)$$

Equation 4.28 represents eigenvalues of the eigenstate ψ_n which is normalized.

$$\int_{-\infty}^{+\infty} \psi_n \psi_m dx = \delta_{nm} \quad (4.30)$$

We can define [5],

$$\int_{-i}^{+\infty} \psi_n x \psi_m dx = \sqrt{\frac{\hbar}{2m\omega}} (\sqrt{m} \delta_{n,m-1} + \sqrt{m+1} \delta_{n,m+1})$$

$$\delta_{nm} = x_{nm} = \sqrt{\frac{\hbar}{2m\omega}} (\sqrt{m} \delta_{n,m-1} + \sqrt{m+1} \delta_{n,m+1}) \quad (4.31)$$

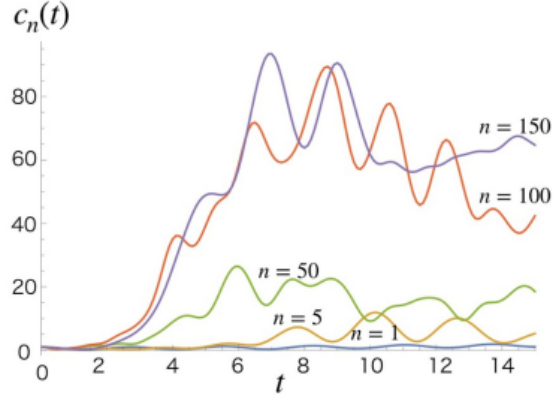


Figure 4.1: Microcanonical OTOC for Harmonic Oscillator [6]

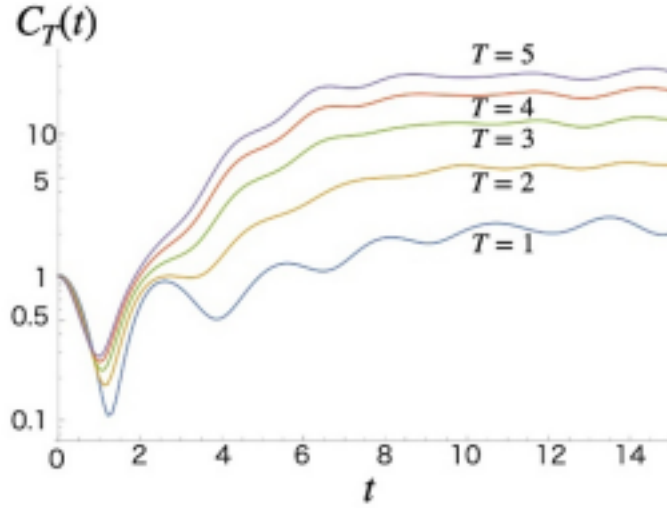


Figure 4.2: Thermal OTOC for Harmonic Oscillator [6]

And,

$$b_{nm}(t) = \delta_{nm} \cos(\omega t)$$

Here, b is a symmetric matrix and $b_{nm}(t)$ is real,
So, the microcanonical OTOC will be [6],

$$C_n(t) = \cos^2 \omega t \quad (4.32)$$

The thermal average will be the same,

$$C_T(t) = \cos^2 \omega t \quad (4.33)$$

4.4 Particle in a 1D box

The Hamiltonian for a particle in a one dimensional box is define as,

$$H = p^2 + V_{box}(x) \quad (4.34)$$

$$V_{box}(x) = \begin{cases} 0 & \text{if } 0 < x < 1 \\ \infty & \text{otherwise} \end{cases}$$

Inside the box the Schrodinger equation is written as,

$$\frac{\partial^2 \psi}{\partial x^2} + \frac{2m}{\hbar}(E - V)\psi = 0 \quad (4.35)$$

Inside the box potential is zero. So, $V = 0$.

$$\frac{\partial^2 \psi}{\partial x^2} + \frac{2m}{\hbar}E\psi = 0 \quad (4.36)$$

Let,

$$k^2 = \frac{2mE}{\hbar} \quad (4.37)$$

$$\frac{\partial^2 \psi}{\partial x^2} + k^2\psi = 0 \quad (4.38)$$

The general solution of the differential equation is,

$$\psi = A \cos kx + B \sin kx \quad (4.39)$$

The boundary condition of the system is $x = 0$, $\psi = 0$. Then from the equation 4.39 we get,

$$0 = A \cos 0 + B \sin 0$$

$$0 = A + 0$$

And,

$$A = 0$$

Putting the value $A = 0$ on the equation 4.39 we get,

$$\psi = B \sin kx \quad (4.40)$$

And the second boundary condition of the system is $x = 1, \psi = 0$. So, equation 4.40 gives us,

$$0 = B \sin k$$

$$\sin k = 0$$

$$\sin k = \sin n\pi$$

Here, $n = 1, 2, 3, \dots$

$$k = n\pi$$

After putting this value on equation 4.40 we get,

$$\psi_n = B \sin(n\pi x) \quad (4.41)$$

To find the eigenfunction, we need to find the value of B which is normalizing factor of ψ .

So,

$$\int_0^1 \psi \psi^* dx = 1 \quad (4.42)$$

From equation 4.41 and 4.42,

$$B^2 \int_0^1 \sin^2(n\pi x) dx = 1$$

$$B^2 \int_0^1 \frac{1 - \cos(2n\pi x)}{2} dx = 1$$

$$\frac{B^2}{2} \int_0^1 (1 - \cos(2n\pi x)) dx = 1$$

$$\frac{B^2}{2} [x]_0^1 - [\sin(2n\pi x)]_0^1 (2n\pi) = 1$$

$$\frac{B^2}{2} (1 - 0) = 1$$

$$B^2 = 2$$

$$B = \sqrt{2}$$

From the equation 4.41 we get the eigenfunction, which is

$$\psi_n = \sqrt{2} \sin(n\pi x) \quad (4.43)$$

Now, we need to find the eigenvalues of the system. From equation 4.37

$$k^2 = \frac{2mE}{\hbar^2}$$

$$E = \frac{\hbar^2 k^2}{2m}$$

$$E = \frac{\hbar^2 \pi^2 n^2}{2m}$$

$$E = \frac{\hbar^2}{2m} \pi^2 n^2 \quad (4.44)$$

Here, the equation 4.44 represents the eigenfunction of particle in a 1-D box.

Chapter 5

OTOC-2

5.1 Circle Billiard

Let us consider a free 2D quantum particle within a disk with radius $R = \frac{1}{\sqrt{\pi}}$, the center of which serves as the origin of our coordinate system. Our boundary condition is that the wave function $\psi(x, y) = 0$ and $x^2 + y^2 = R^2$ in Cartesian coordinates x and y .

The Hamiltonian of a circle billiard is ,

$$H = p_1^2 + p_2^2 + V_{cir}(x_1, x_2) \quad (5.1)$$

$$V_{cir}(x, y) = \begin{cases} 0 & \text{if } x^2 + y^2 < R^2 \\ \infty & \text{otherwise} \end{cases}$$

To make our problem simple, we consider the system in polar coordinate (r, θ) instead of cartesian (fig: 5.1).

Here,

$$x = r \cos \theta$$

$$y = r \sin \theta$$

The 1-D time dependent Schrodinger equation is,

$$\frac{-\hbar^2}{2m} \frac{\partial^2 \psi}{\partial x^2} + V\psi = \frac{-\hbar}{i} \frac{\partial \psi}{\partial t} \quad (5.2)$$

Here,

$$\psi(x, t) = u(x)f(t)$$

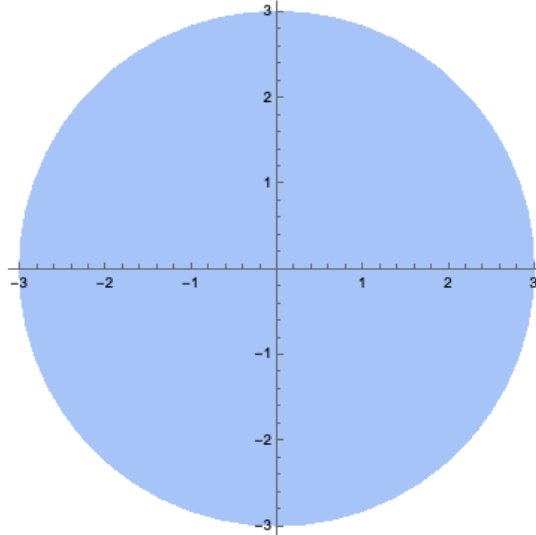


Figure 5.1: Implicit region of a circle

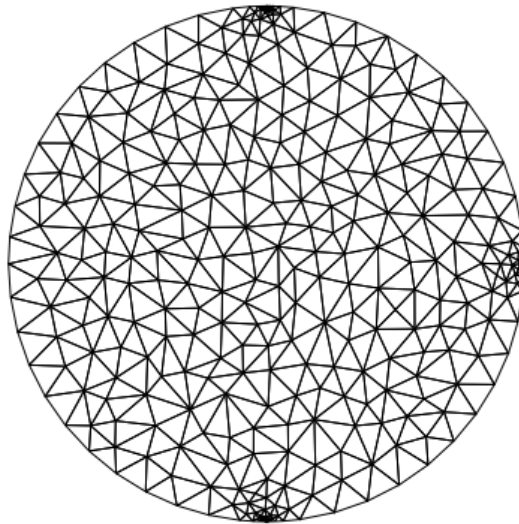


Figure 5.2: Mesh of a circle billiard

Then, equation 5.2 implies,

$$\frac{-\hbar^2 d^2u}{2m dx^2} f + Vuf = \frac{-\hbar df}{i dt} u \quad (5.3)$$

$$\frac{-\hbar^2 d^2u}{2m dx^2} \frac{1}{u} + V = \frac{-\hbar df}{i dt} \frac{1}{f}$$

$$\frac{-\hbar^2 d^2u}{2m dx^2} \frac{1}{u} + V = E$$

Because,

$$E = \frac{-\hbar}{i} \frac{df}{dt} \frac{1}{f}$$

$$\frac{-\hbar^2}{2m} \frac{1}{u} \frac{d^2u}{dx^2} + V - E = 0$$

So,

$$\frac{d^2u}{dx^2} + \frac{2m}{\hbar^2}(E - V)u = 0 \quad (5.4)$$

In three dimensional system we can replace d with Laplacian operator ∇ ,

$$\nabla^2 u + \frac{2m}{\hbar^2}(E - V)u = 0 \quad (5.5)$$

If we replace $u(x)$ by $\psi(r, \theta)$, the equation 5.5 will be,

$$\nabla^2 \psi + \frac{2m}{\hbar^2}(E - V)\psi = 0 \quad (5.6)$$

As we know,

$$\nabla^2 = \frac{1}{r} \frac{\partial}{\partial r} \left(r \frac{\partial}{\partial r} \right) + \frac{1}{r^2} \frac{\partial^2}{\partial \theta^2}$$

So, in two dimensional polar coordinate the Schrodinger equation will be [3],

$$\frac{1}{r} \frac{\partial}{\partial r} \left(r \frac{\partial \psi}{\partial r} \right) + \frac{1}{r^2} \frac{\partial^2 \psi}{\partial \theta^2} + \frac{2m}{\hbar^2}(E - V)\psi = 0 \quad (5.7)$$

As this is a separation of variable we can write,

$$\psi(r, \theta) = R(r)\Theta(\theta)$$

The system has also angular symmetry and the angular part $\Theta(\theta)$ has no effect on the system. So,

$$\psi(r, \theta) = \psi(r)e^{in\theta}$$

Then, equation 5.7 becomes,

$$\frac{1}{r} \frac{\partial}{\partial r} r \frac{\partial \psi e^{in\theta}}{\partial r} + \frac{1}{r^2} \frac{\partial^2}{\partial \theta^2} \psi e^{in\theta} + \frac{2mE}{\hbar^2} \psi e^{in\theta} = 0$$

$$\frac{1}{r} \frac{\partial}{\partial r} r \frac{\partial}{\partial r} \psi - \frac{n^2}{r^2} \psi + \frac{2mE}{\hbar} \psi = 0$$

$$\frac{1}{r} \frac{\partial^2}{\partial r^2} \psi + \frac{1}{r} \frac{\partial}{\partial r} \psi - \frac{n^2}{r^2} \psi + \frac{2mE}{\hbar} \psi = 0$$

$$\left(\frac{1}{r} \frac{\partial^2}{\partial r^2} + \frac{1}{r} \frac{\partial}{\partial r} - \frac{n^2}{r^2} \right) \psi + \frac{2mE}{\hbar} \psi = 0 \quad (5.8)$$

Put, $k^2 = \frac{2mE}{\hbar}$ on equation 5.8

$$\left(\frac{\partial^2}{\partial r^2} + \frac{1}{r} \frac{\partial}{\partial r} \right) \psi + k^2 \psi - \frac{n^2}{r^2} \psi = 0$$

$$\left[\frac{\partial^2}{\partial r^2} + \frac{1}{r} \frac{\partial}{\partial r} + \left(\frac{k^2 r^2 - n^2}{r^2} \right) \right] \psi = 0$$

$$r^2 \frac{\partial^2}{\partial r^2} \psi + r \frac{\partial}{\partial r} \psi + (k^2 r^2 - n^2) \psi = 0 \quad (5.9)$$

Now,

$$\psi(r) = a_n J_n(kr) + b_n Y_n(kr)$$

Here,

$J_n = \text{First kind Bessel function}$

$Y_n = \text{Second kind Bessel function}$

At $r = 0$ the second kind Bessel function $Y_n \rightarrow \infty$

So,

$$\psi(r) = a_n J_n(kr)$$

Therefore, the general solution becomes,

$$\psi_{nl} = N J_{nl} \sqrt{\pi} \beta_{nl} r e^{in\theta} \quad (5.10)$$

In this equation, N is normalizing factor and β_{nl} represents zeros of Bessel function. And l is the l^{th} zero of J_n .

At $r = R$ the eigenfunction $\psi(R, \theta) = 0$.

So,

$$J_n(kR) = 0$$

$$kR = \beta_{nl}$$

$$k^2 = \left(\frac{\beta_{nl}}{R}\right)^2$$

$$\frac{2mE}{\hbar} = \left(\frac{\beta_{nl}}{R}\right)^2$$

$$E = \frac{\hbar}{2mE} \left(\frac{\beta_{nl}}{\frac{1}{\sqrt{\pi}}}\right)^2$$

$$E_{nl} = \frac{\hbar}{2mE} \pi \beta_{nl}^2 \tag{5.11}$$

Equation 5.11 represents the eigenvalue of the system. We use Mathematica to find eigenvalues for different values of n shows in (fig: 5.3)

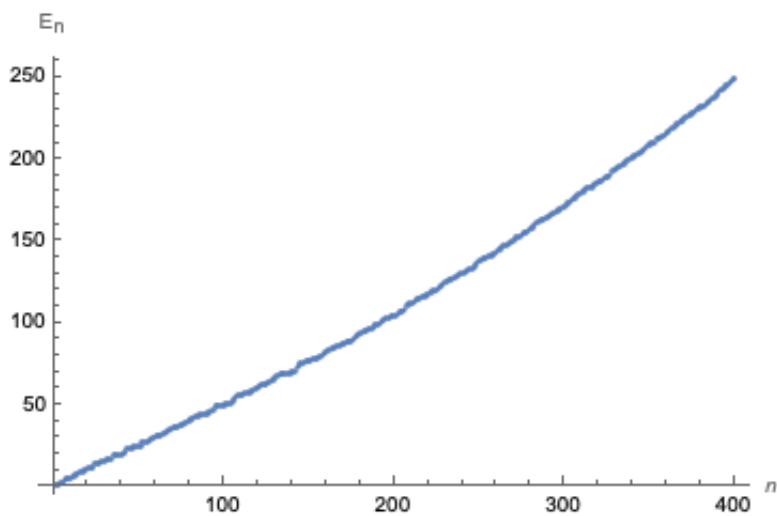


Figure 5.3: Eigenvalues of the circle billiard

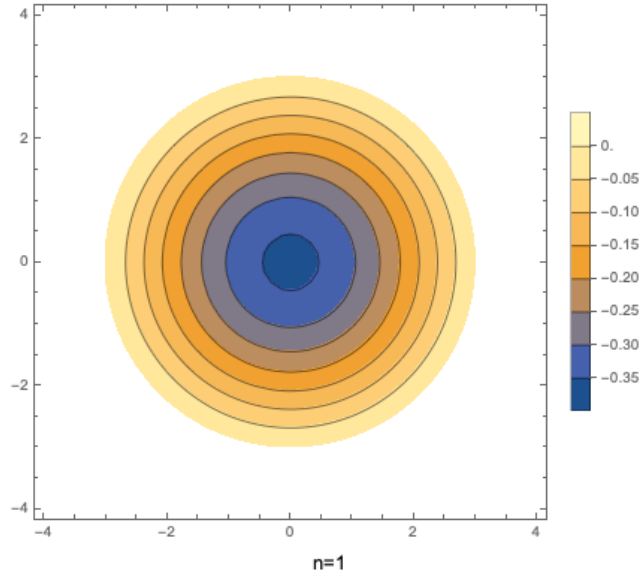


Figure 5.4: Eigenfunction for $n = 1$ of circle billiard

Now, we need to find the matrix elements of x

$$x_{nm} = \int_0^R r dr \int_0^{2\pi} \psi_n^* x \psi_m d\theta$$

In this system, $R = \frac{1}{\sqrt{\pi}}$ and $x = r \cos \theta$

$$x_{nm} = \int_0^{\frac{1}{\sqrt{\pi}}} r dr \int_0^{2\pi} \psi_n^* r \cos \theta \psi_m d\theta \quad (5.12)$$

Equation 5.12 represents the matrix elements of x .

Fig: 5.4 shows eigenfunction for $n = 1$

Fig: 5.5 shows eigenfunction for $n = 2$

Fig: 5.6 shows eigenfunction for $n = 3$

Fig: 5.7 shows eigenfunction for $n = 6$

Fig: 5.8 shows eigenfunction for $n = 10$

Fig: 5.9 shows eigenfunction for $n = 50$

Fig: 5.10 shows eigenfunction for $n = 100$

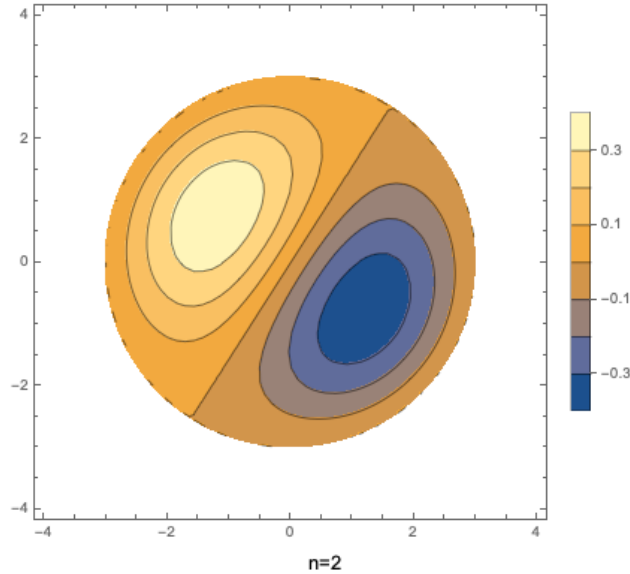


Figure 5.5: Eigenfunction for $n = 2$ of circle billiard

Fig: 5.11 shows eigenfunction for $n = 200$

Fig: 5.12 shows eigenfunction for $n = 400$

We can see the three dimensional view for $n = 400$ in fig: 5.13.

5.2 Stadium Billiard

The stadium billiard has been around for more than 45 years. The original spark for research came from Bunimovich's demonstration that the stadium was a B-system. His argument was attained by taking into account border forms for a broad class of billiards devoid of any dispersing elements. Dispersing here refers to paths diverging. Furthermore, the billiard was believed to contain at least one focus because it had previously been established that polygonal shapes with no focusing components have zero entropy. Furthermore, it was believed that the boundary's focusing region would have a constant curve.

Since the interior of the circle points toward the interior of the billiard, the border might be made up of both straight and curved parts. A bundle compresses and then expands after reflection from a circular section, highlighting the stochastic nature of the system and making it difficult to forecast when any subsequent focussing would occur. The proof primarily considers successive reflections of bundles of paths in order to show the B-property. The simplicity with which these entities possessed the B-property led to the proof of the K-property.

Due of the widespread interest these publications garnered, a straightforward example of the type of things covered in them, the stadium, is frequently referred to as the Bunimovich stadium. The K-property suggests that the object has positive entropy, which is why the papers are so significant. This entropy is supposedly constant practically everywhere, according to the B-property.

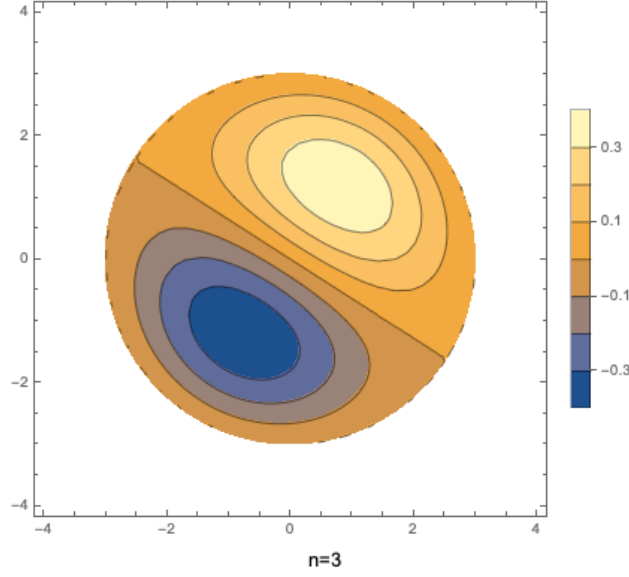


Figure 5.6: Eigenfunction for $n=3$ of circle billiard

Hamiltonian of a stadium billiard is

$$H = p_1^2 + p_2^2 + V_{stad}(x, y) \quad (5.13)$$

Where,

$$V_{stad}(x) = \begin{cases} 0 & \text{if } (x, y) \in \Omega \\ \infty & \text{otherwise} \end{cases}$$

Here, Ω is the region of the stadium where the radius of the semicircle is R so the width of the stadium is $2R$ and the length of the implicit rectangle is $2a$.

A free particle can move inside the region in it reflect when it get at boundary and shows a trajectory line (fig: 5.14). The sensitivity to beginning conditions is one of chaotic systems' most distinctive behaviors that means if we change a little bit in initial condition the the system will show a huge change in latter time.

We can denote the phase of the particle in stadium billiard by $x(t)$. If we change a little in the phase space by $\delta(t)$ then the final phase space will be,

$$x(t) + \delta(t)$$

Because of the chaotic behaviour of the system the tiny change $\delta(t)$ grows exponentially in future and we can define the change by lyapunov exponent (fig: 5.15). which become,

$$x(t) = e^{\lambda t}$$

here, λ is lyapunov exponent and indicates the exponential growth of the initial change.

If the velocity of the particle inside the stadium is v and the surface area of the stadium shape billiard is A then [4],

$$\lambda = \frac{v}{\sqrt{A}} \quad (5.14)$$

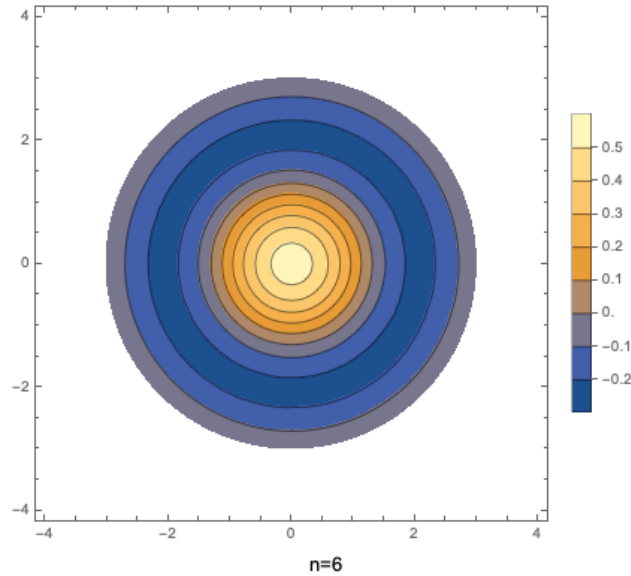


Figure 5.7: Eigenfunction for $n = 6$ of circle billiard

We need to recall the time independent Schrodinger equation for quantum stadium billiard.

$$-\nabla^2\psi_n + V_{stad}\psi_n = E_n\psi_n \quad (5.15)$$

fig: 5.16 shows the Mesh region of stadium billiard.

It is very difficult to solve stadium billiard problem without computer system. To solve this we use Mathematica to find eigenvalues of the system. To do this we take $\frac{a}{R} = 1$ in (fig 5.17) shows the eigenvalues of stadium billiard
To find eigenfunction of stadium billiard we take help of Mathematica.

Fig: 5.18 shows eigenfunction for $n = 1$

Fig: 5.19 shows eigenfunction for $n = 2$

Fig: 5.20 shows eigenfunction for $n = 3$

Fig: 5.21 shows eigenfunction for $n = 10$

Fig: 5.22 shows eigenfunction for $n = 50$

Fig: 5.23 shows eigenfunction for $n = 100$

Fig: 5.24 shows eigenfunction for $n = 200$

Fig: 5.25 shows eigenfunction for $n = 400$

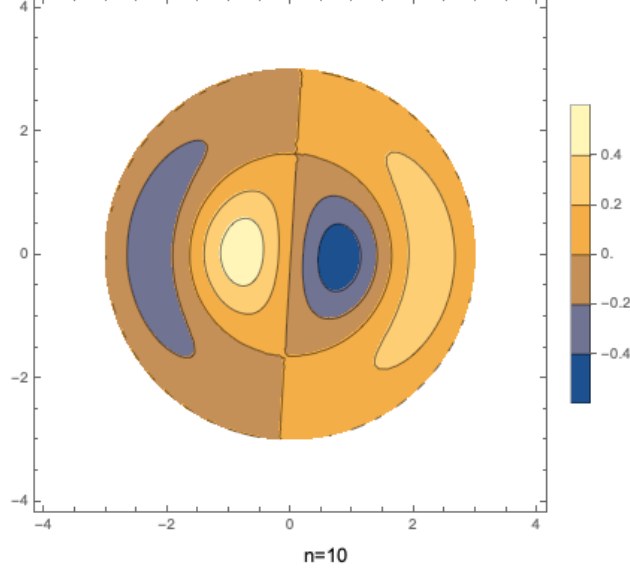


Figure 5.8: Eigenfunction for $n = 10$ of circle billiard

We can see the three dimensional view for $n = 400$ in fig: 5.26

5.3 Classical Statistics

In two dimensional phase space, the OTOC is written as [4],

$$C(t) = \frac{1}{Z} \int \frac{1}{2\pi} e^{-\beta H} \{x(t), p(0)\}^2 dx dp \quad (5.16)$$

In this equation 5.16, Z is partition function,

$$Z = \int \frac{1}{2\pi} e^{-\beta H} dx dp$$

and $\{..,..\}$ represents the poisson bracket.// When a particle stay inside the region the potential remain zero and can move freely. When it reach at the boundary the particle bounce back.

At boundary,

$$p(t) = -p(t)$$

If we change a tiny δx at starting position $x(0) + \delta x(0)$ it appears after n number of bounce and time t as

$$\delta x(t) = (-1)^n \delta x(0) \quad (5.17)$$

In equation 5.17 we can see that, $\delta x(t)$ depends on $(-1)^n$

So, poisson bracket will be,

$$\{x(t), p(0)\} = \frac{\delta(t)}{\delta(0)}$$

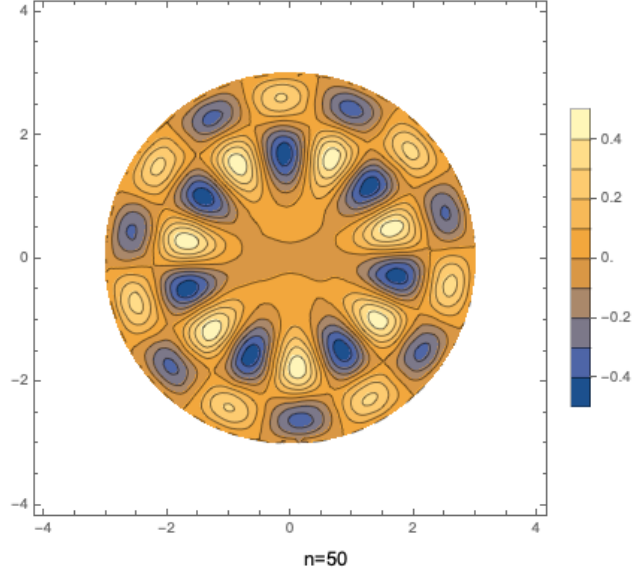


Figure 5.9: Eigenfunction for $n = 50$ of circle billiard

$$\{x(t), p(0)\} = (-1)^n$$

After putting this value on equation 5.16 we get,

$$C(t) = \frac{1}{Z} \int \frac{1}{2\pi} e^{-\beta H} \{(-1)^n\}^2 dx dp \quad (5.18)$$

We can find the OTOC for stadium billiard classically [4]

$$C = t e^{Tt^2}$$

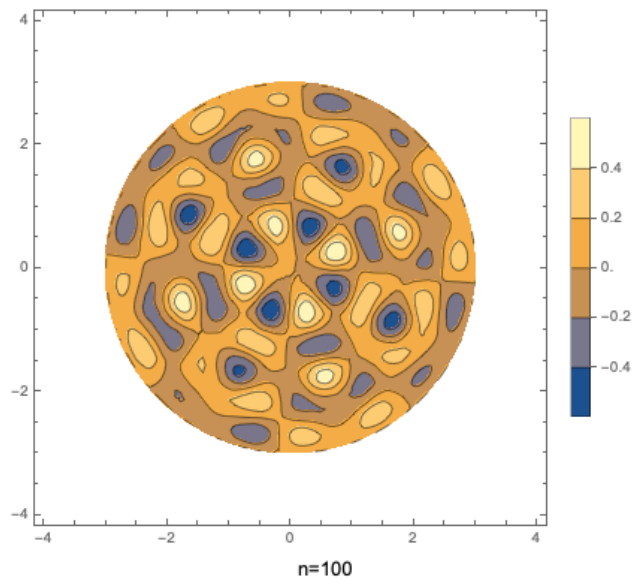


Figure 5.10: Eigenfunction for $n = 100$ of circle billiard

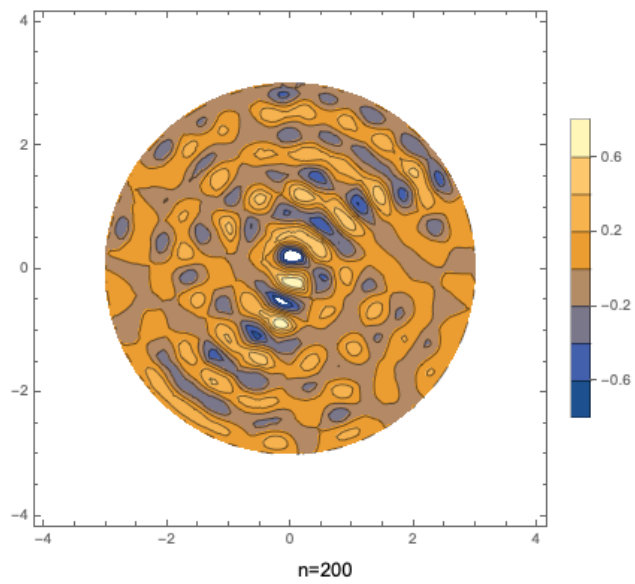


Figure 5.11: Eigenfunction for $n = 200$ of circle billiard

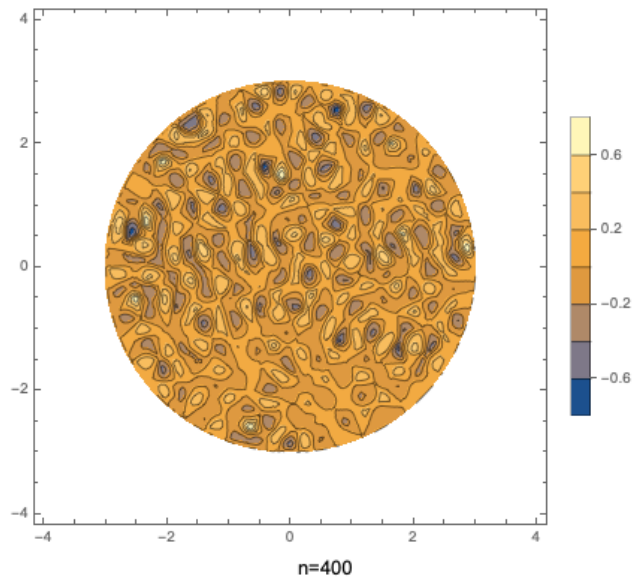


Figure 5.12: Eigenfunction for $n = 400$ of circle billiard

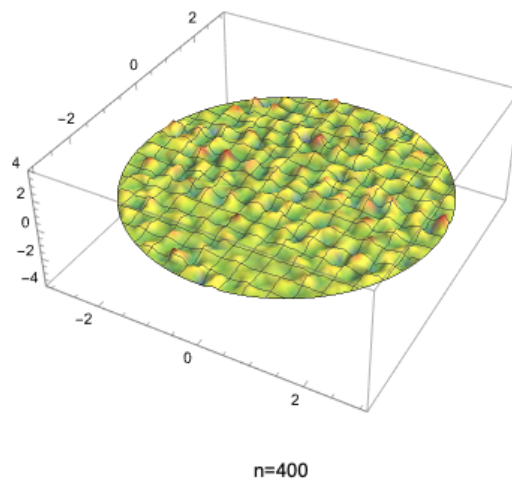


Figure 5.13: 3D view for $n = 400$ in circle billiard

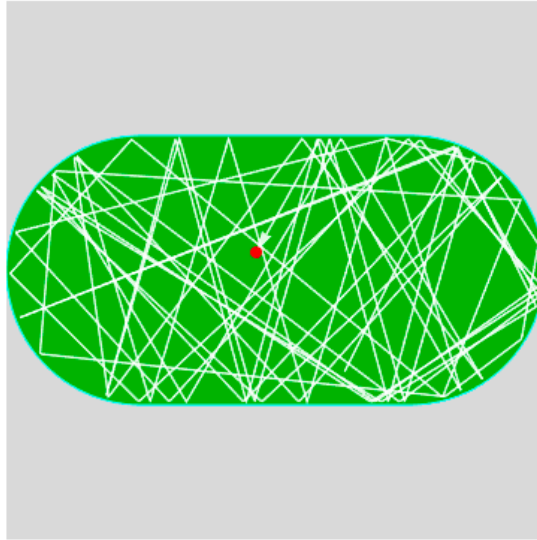


Figure 5.14: Trajectory of stadium billiard

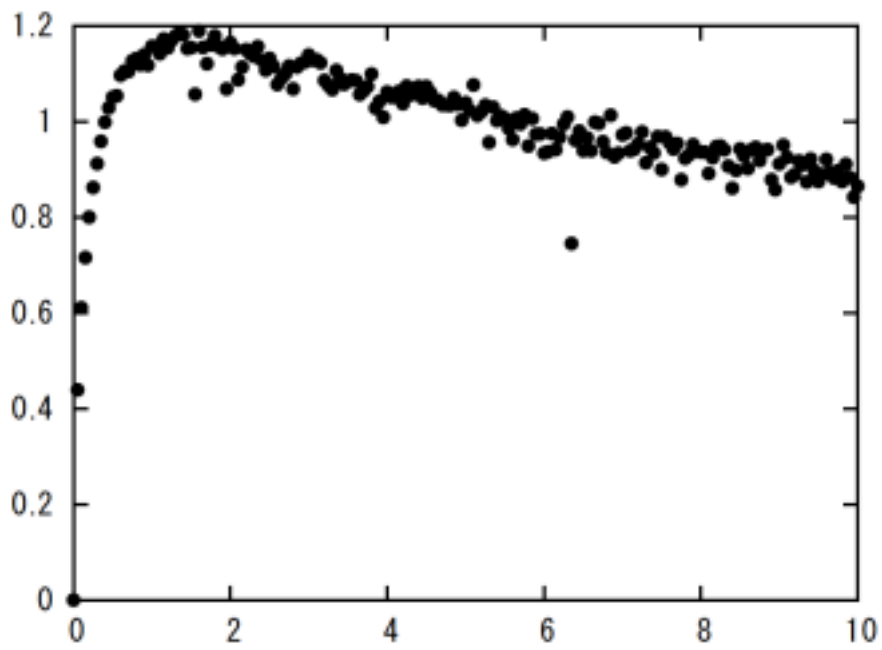


Figure 5.15: Positive Lyapunov exponent

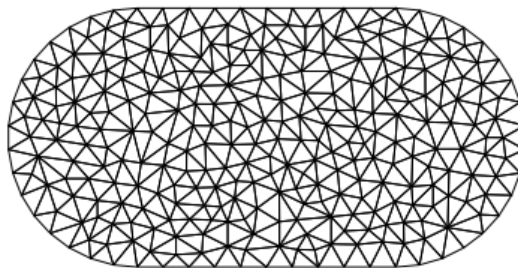


Figure 5.16: Mesh of stadium billiard

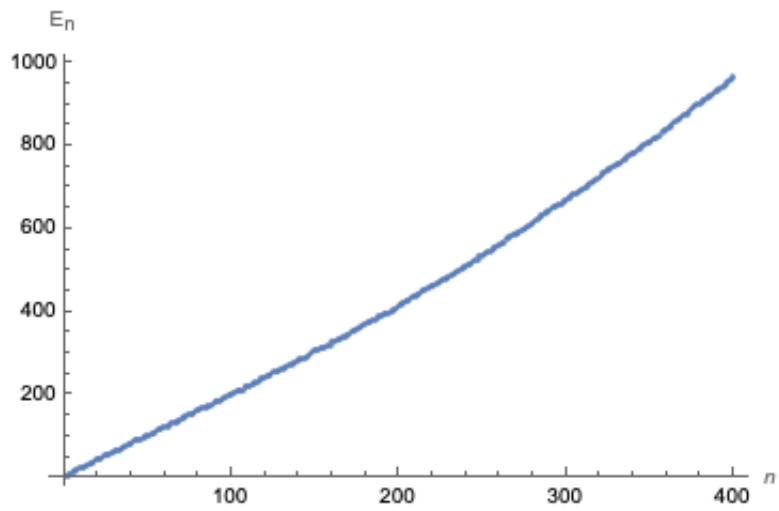


Figure 5.17: Eigenvalues of stadium billiard

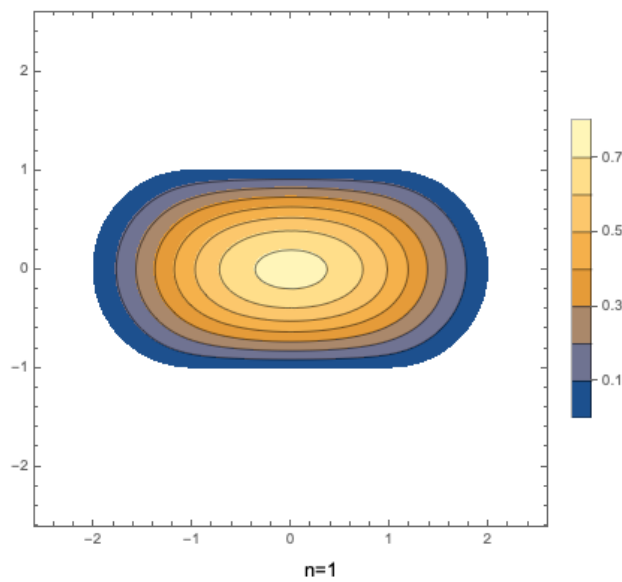


Figure 5.18: Eigenfunction for $n=1$ of stadium billiard

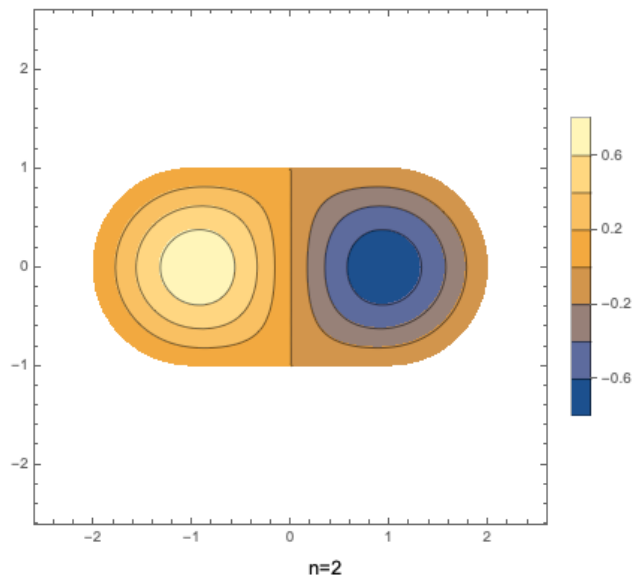


Figure 5.19: Eigenfunction for $n=2$ of stadium billiard

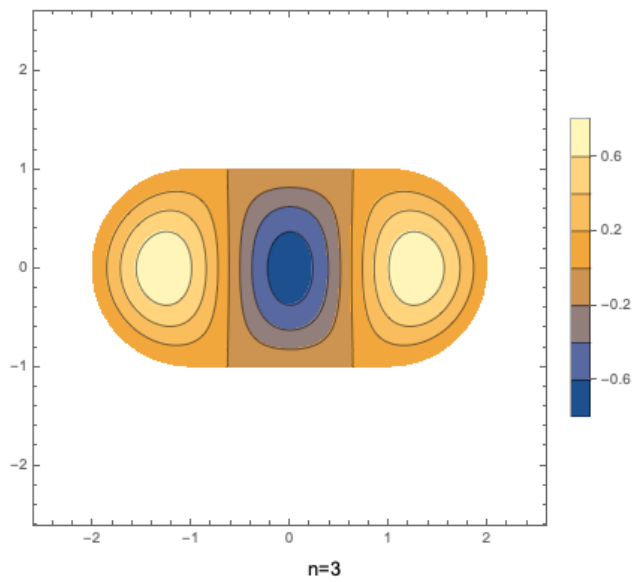


Figure 5.20: Eigenfunction for $n=3$ of stadium billiard

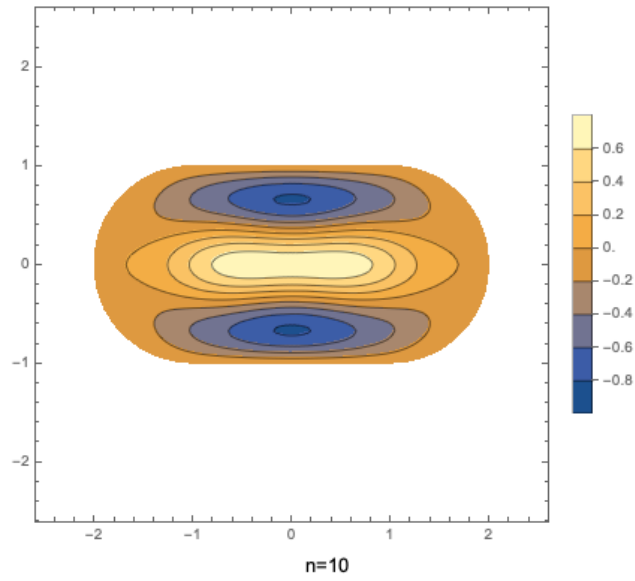


Figure 5.21: Eigenfunction for $n=10$ of stadium billiard

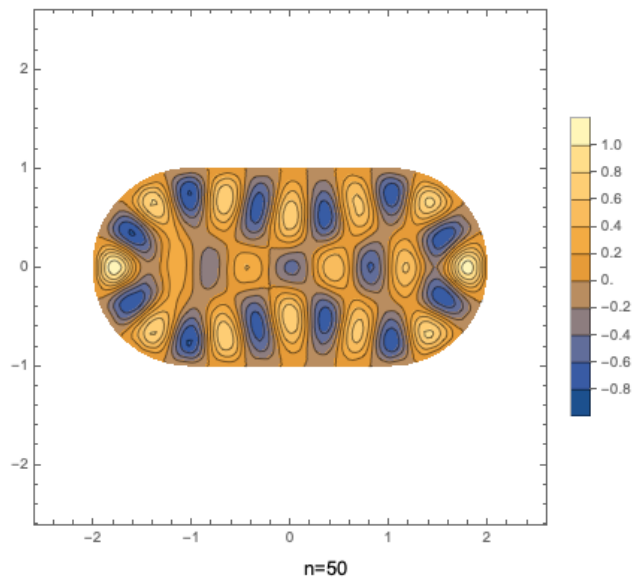


Figure 5.22: Eigenfunction for $n=50$ of stadium billiard

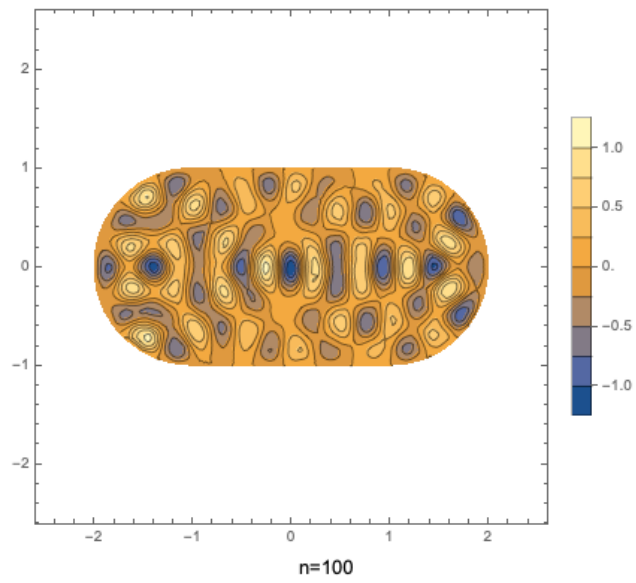


Figure 5.23: Eigenfunction for $n=100$ of stadium billiard

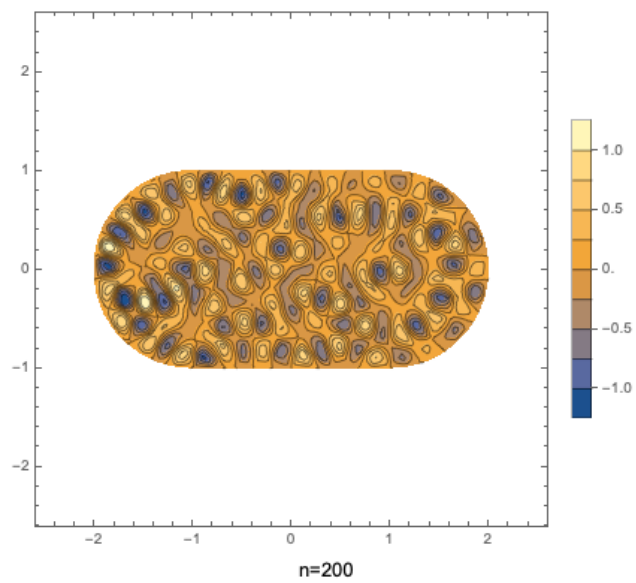


Figure 5.24: Eigenfunction for $n=200$ of stadium billiard

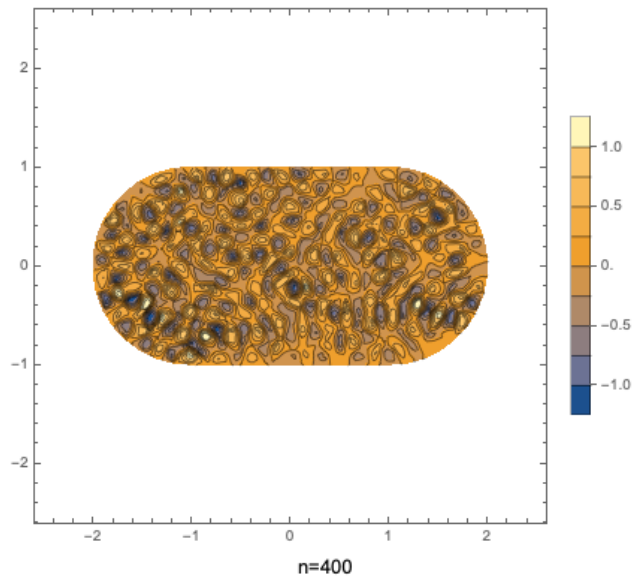


Figure 5.25: Eigenfunction for $n=400$ of stadium billiard

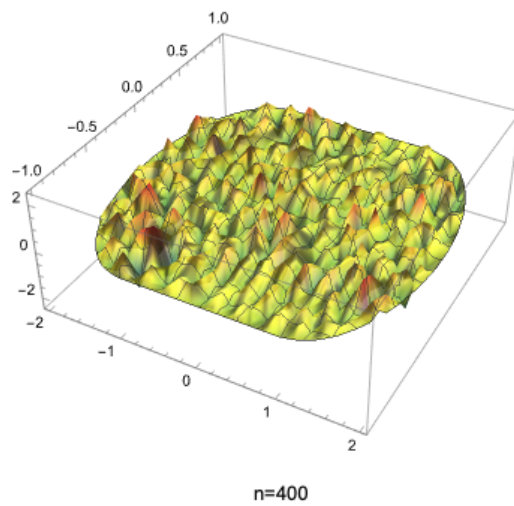


Figure 5.26: 3D view for $n= 400$ in stadium billiard

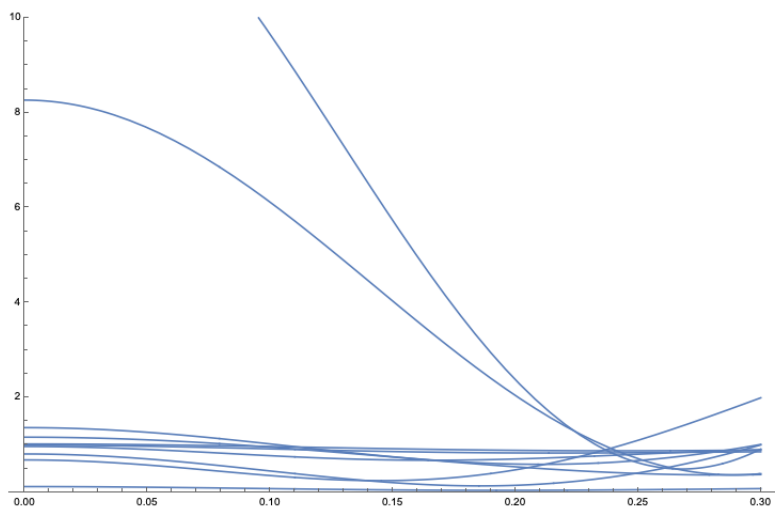


Figure 5.27: OTOC for Stadium billiard

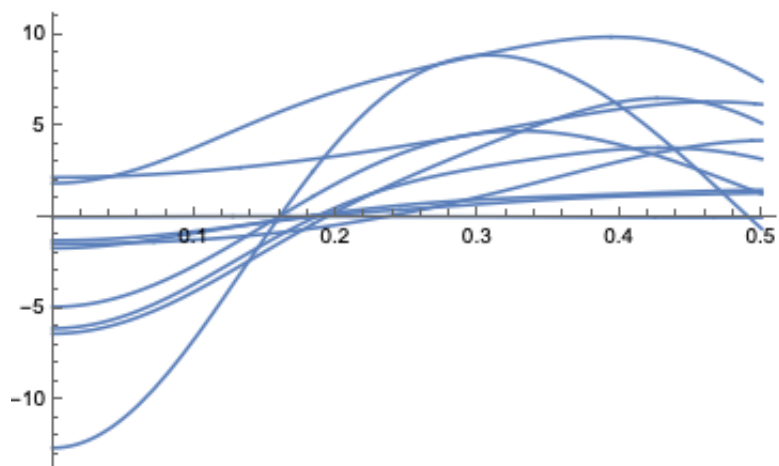


Figure 5.28: OTOC for Stadium billiard

Chapter 6

Conclusion

In this thesis, we have looked at the idea of quantum chaos and certain systems that display it. The exponential expansion is not seen in the stadium billiard OTOC. The spectral form factor was indirectly motivated as a tool to study the discrete spectra of quantum chaotic systems and compare them to random matrix theory ensembles. In contrast, the OTOC was directly motivated by the Poisson bracket argument that showed how quantum chaotic systems would be expected to behave. For different temperatures and energy levels, we numerically determined the microcanonical OTOC and the thermal OTOC of the nonlinearly linked harmonic oscillator.

In addition, we discovered that the quantum mechanics for the particle in a one-dimensional box and the classical statistics for the OTOC do not coincide. In this paper, we discussed the Lyapunov exponent's behaviour and its application and implementation in a chaotic system. In addition, we discovered the Eigenvalues of circle and stadium billiards. Besides this, we showed the trajectory of a particle inside a stadium-shaped billiard.

There is still much to be studied in the context of straightforward quantum mechanics, especially for systems with continuous spectra. There don't seem to be conclusive findings linking classical and quantum chaos.

Bibliography

- [1] T. Bountis, “Fundamental concepts of classical chaos i,” *Physical Review E*, vol. 100, no. 4, 1995/04/01 1995. DOI: 10.1007/BF02228810. [Online]. Available: <https://doi.org/10.1007/BF02228810>.
- [2] M. A. Porter, “An introduction to quantum chaos,” vol. 2, 2001. DOI: 10.48550/ARXIV.NLIN/0107039.
- [3] L. Nanni, *The hydrogen atom: A review on the birth of modern quantum mechanics*, 2015. DOI: 10.48550/ARXIV.1501.05894. [Online]. Available: <https://arxiv.org/abs/1501.05894>.
- [4] K. Hashimoto, K. Murata, and R. Yoshii, “Out-of-time-order correlators in quantum mechanics,” *Journal of High Energy Physics*, vol. 2017, no. 10, Oct. 2017. DOI: 10.1007/jhep10(2017)138. [Online]. Available: <https://doi.org/10.1007%2Fjhep10%282017%29138>.
- [5] A. Resnick, “Quantum mechanics, by richard fitzpatrick,” *Contemporary Physics*, vol. 59, no. 1, pp. 73–74, 2018. DOI: 10.1080/00107514.2017.1381169. eprint: <https://doi.org/10.1080/00107514.2017.1381169>. [Online]. Available: <https://doi.org/10.1080/00107514.2017.1381169>.
- [6] T. Akutagawa, K. Hashimoto, T. Sasaki, and R. Watanabe, “Out-of-time-order correlator in coupled harmonic oscillators,” *Journal of High Energy Physics*, vol. 2020, no. 8, Aug. 2020. DOI: 10.1007/jhep08(2020)013. [Online]. Available: <https://doi.org/10.1007%2Fjhep08%282020%29013>.